Adsorption Dynamics of Alkanes on Single-Wall Carbon Nanotubes: A Molecular Beam Scattering Study

S. Funk[†] and U. Burghaus*[,†]

Department of Chemistry and Molecular Biology, North Dakota State University, Fargo, North Dakota 58105-5516

Brian White,[‡] Stephen O'Brien,[£] and Nicholas J. Turro[‡]

Department of Chemistry, Columbia University, New York, New York 10027, and Department of Applied Physics and Applied Mathematics, Columbia University, New York, New York 10027

Received: January 23, 2007; In Final Form: March 20, 2007

The adsorption dynamics of *n*-/isobutane on "closed"-end (as-prepared, c-CNTs) and open-end (vacuum-annealed) carbon nanotubes (o-CNTs) have been studied by molecular beam scattering adsorption probability measurements. Thermal desorption spectroscopy (TDS) and scanning electron microscopy have been used to characterize the CNTs. Evident from TDS data, o-CNTs allow internal adsorption sites to be populated, which is correlated with an increase in the initial adsorption probabilities as compared with c-CNTs, consistent with the enhancement in the surface area by opening the tube ends. Furthermore, precursor-mediated adsorption dynamics were observed.

1. Introduction

The economic potential of nanotubes (NTs) was explored shortly after the discovery of carbon nanotubes (CNTs).[1] Material science applications (at ambient pressures) such as composite materials,[2] sensors,[3,4] gas capture,[5,6] and nanoelectronics[7−9] have been extensively studied. However, rather little attention has been paid to applications in heterogeneous catalysis,[10−12] particularly in ultrahigh vacuum (UHV) surface chemistry model studies, although the advantages of CNTs as supports for fuel cells[13,14] and the Fischer−Tropsch[15,16] synthesis have been demonstrated. The few UHV surface chemistry studies conducted so far focus on the application of kinetic and spectroscopic techniques.[17−20] Gas-surface energy-transfer mechanisms (adsorption dynamics), which are a prerequisite for any adsorption process, are fairly unexplored.[10−12] Although initial adsorption probabilities can be obtained (at low impact energies of the gas-phase species) by thermal desorption spectroscopy (TDS),[21] the experimental technique of choice to study the adsorption dynamics is molecular beam scattering. However, we are not aware of any molecular beam scattering studies conducted on a nanotube system. Improvements on a large variety of applications require detailed knowledge about the gas−nanotube interaction in order to enable a functionalization and modification of CNTs for catalysis and material science (i.e., gas sensors).

Studies of the adsorption of hydrocarbons have a long-standing tradition in surface chemistry due to their importance as building blocks in the petroleum industry. For example, TDS studies characterizing the adsorption kinetics of alkanes have been conducted for a large variety of single-crystal surfaces, including graphite,[22−24] sapphire,[25] ZnO,[26] Ru,[27] Cu,[28] alloys,[29] and silica.[30] At low exposures, the alkanes form a monolayer, providing information about kinetics parameters (which can reflect specific adsorption sites)[31] and lateral interactions.[32] At large exposures, the multilayer grows with desorption temperatures independent of the surface, allowing for a simple calibration of the temperature reading in TDS. As a unique feature of CNTs, the adsorption on grooves, external, and internal sites can be distinguished with TDS providing "fingerprint spectra", uniquely indicating high-energy binding sites[6] and gas adsorption on interior sites.[33] The adsorption of pentane, nonane, trimethylpentane, Xe, CF_4, water, O_2, CCl_4, CO_2, and NO have so far been studied at UHV conditions on CNTs, mostly by means of TDS and infrared spectroscopy.[17−19,21,33] We are not aware of surface chemistry studies of butane on CNTs.

The adsorption dynamics of alkanes have been investigated by molecular beam scattering on metal and metal oxide surfaces by means of adsorption probability measurements mapping the potential energy surface (see, e.g., refs 26 and 28). For most systems, molecular and precursor-mediated adsorption is present, that is, the coverage (surface particle density)-dependent adsorption probability, $S(\Theta)$, remains approximately independent of the coverage, Θ, since the gas-phase species are trapped in extrinsic (above occupied sites) and/or intrinsic (above clean sites) precursor states as a prerequisite for adsorption. At low adsorption temperatures, T_{ads}, and large impact energies, $S(\Theta)$ often increases with Θ, that is, adsorbates assist the adsorption of gas-phase species (adsorbate-assisted adsorption).[26] Without precursor states, $S(\Theta)$ decreases linearly with Θ (Langmuirian adsorption dynamics). For a few metal surfaces, bond activation has been observed (see, e.g., ref 34).

In this study, we compare the adsorption kinetics and dynamics of *n*-/isobutane on "closed" (as-prepared, c-CNTs)

* To whom correspondence should be addressed. E-mail: uwe.burghaus@ndsu.edu. URL: www.chem.ndsu.nodak.edu. Fax: 701-231-8831.

[†] North Dakota State University.

[‡] Department of Chemistry, Columbia University.

[£] Department of Applied Physics and Applied Mathematics, Columbia University.

10.1021/jp070595l CCC: $37.00
Published on Web 05/11/2007

and UHV-annealed, open-end carbon nanotubes (o-CNTs). TDS data indicate that the c-CNTs are already fairly clean but with the tube ends blocked with residuals (functionalities) originating from the solvents used to prepare the samples.[35] Evident from TDS data, UHV-annealed o-CNTs allow internal adsorption sites to be populated, which is correlated with an increase in the initial adsorption probabilities, consistent with the enhancement in the surface area by opening the tube ends. Furthermore, precursor-mediated (Kisliuk-like) adsorption dynamics have been observed for the o-CNTs, whereas the as-prepared c-CNTs show more Langmuirian-like (direct) adsorption dynamics. To distinguish possible support and CNT effects, the adsorption of the alkanes has also been studied thoroughly on clean silica supports,[32] and pentane/CNT data are included as a reference system.[33]

2. Experimental Procedures

2.1. Materials. Single-walled carbon nanotube solutions were prepared using a method by O'Connell, et al.[36] Commercially available CNTs, grown by the high-pressure CO (HiPco) method from Carbon Nanotechnologies Inc., were mixed with a 1% w/v solution of sodium dodecyl sulfate (SDS) in deionized water. The mixture was subjected to vigorous sonication (using a sonication probe, Branson Sonifier 450) and centrifugation at 100 000g for 4.5 h. The sonication exfoliates the nanotube bundles, while the centrifugation removes the remaining bundles and other impurities including catalyst and carbonaceous particles.[36] The supernatant consists of short, isolated, single-wall CNTs, as confirmed by absorption and fluorescence spectroscopy as well as atomic force microscopy.[37] A 10 × 10 mm p-type silicon wafer with a 300 nm thick oxide layer (bluish color) was cleaned by sonicating in acetone, then ethanol, and drying with compressed air. The surface of the wafer was covered with the nanotube solution and allowed to dry for several hours on the bench top. Two additional coatings were added to increase the CNT density. In total, ~600 μg of the suspension consisting of an estimated 200 μg of CNTs have been deposited. Smaller amounts of CNTs did not reveal clear nanotube effects in TDS and beam scattering measurements. Once dry, the wafer was heated under N_2 to 600 K at 20 K/min and annealed for 30 min in a thermogravimetric analysis instrument (TA Instruments TGA Q50) in order to remove the SDS surfactant. Under these conditions, the alkane backbone of the SDS molecule was easily removed, but some Na_2SO_4 crystals remained on the surface of the sample, as determined by energy-dispersive X-ray diffraction. Scanning electron microscopy (SEM) images and energy-dispersive X-ray diffraction data were obtained on an Hitachi 4700 field emission SEM. It is confirmed by the presented TDS data (see below) that the CNTs have open ends due to the vigorous sonication that cuts the nanotubes and exfoliate the bundles. The CNTs supported on silica were annealed for 15 min at 450 K in ultrahigh vacuum (UHV), which removed remaining functionalities and opened the tube-ends (see section 3.1).[38] It has been shown by others that HiPco-produced CNTs have an average diameter of 13.6 Å.[39] Thus, adsorption of iso/*n*-butane (maximum C−C distance = 5.5 Å) on interior sites is expected.

2.2. Measuring Procedures. The measurements have been conducted with a home-built, triply differentially, pumped molecular beam system at North Dakota State University.[40] The supersonic beam is attached to a scattering chamber that contains standard UHV analytical tools including, most importantly for this study, a mass spectrometer (Pfeiffer QME200). The impact energy, E_i, of *n*-/isobutane could be varied within 0.31−1.55 eV by using pure beams and by seeding 3% of the alkanes in He, combined with a variation of the nozzle temperature from 300 to 650 K. For the *n*-pentane measurements, collected as a reference data set,[33] a pure beam (E_i = 0.36 eV) was used. According to the reproducibility and the signal-to-noise ratio of the King and Wells[41] curves, the statistical error in the initial adsorption probabilities, S_0, amounts to ±0.02. For calculating S_0 from the uptake curves, the finite vacuum time constant of the scattering chamber is taken into account. Therefore, the initial transient was ignored, and S_0 was obtained by extrapolating linearly back to the beginning of the reflectivity curve where the beam flag was opened. The adsorption probability curves were smoothed while conserving the shape of the transients. Measurements were taken for normal impact angles.

It is important to note that TDS measurements can be effected by contributions from the sample holder, and so forth. Therefore, a number of precautions have been taken. (1) The mass filter has an 8 mm aperture, and the distance from the sample (10 × 10 mm) to the mass spectrometer amounts to ~2 mm. (2) The sample holder consists of a 4 pin ceramic feed through with the air side connected to a stainless steel rod which acts as the reservoir for liquid N_2. Thus, no bulky parts have been used in designing the sample holder. Helium gas has been bubbled through the liquid N_2, reducing the sample temperature to 85−90 K.[42] (3) For most of the measurements, the alkanes have been dosed on the sample with the molecular beam system, keeping the background pressure while dosing the gas below 2×10^{-8} mbar. The beam flux has been estimated by comparing the area of the TDS peaks obtained by backfilling the chamber with the TDS peak areas detected by molecular beam dosing. This calibration was consistent with TDS results obtained for the silica support (taking the measured adsorption probability into account), which showed a clear condensation peak. The exposures, χ, (i.e., the amount of exposed particles) are given in monolayers (ML, one molecular layer), using a numerical value typical for planar surfaces, that is, 1 ML is defined as 1×10^{15} particles/cm^2. Determining the absolute alkane coverage, which is related to the total surface area of the CNTs, is experimentally challenging.[6,43,44] To provide an estimate, TDS peak areas obtained by condensing butane on the sample backside and on the clean silica support have been compared with the TDS of the CNT/silica sample. (4) TDS reference data for clean silica have been collected.

The CNT/silica samples were mounted on a tantalum plate, permitting radiative and electron beam heating by a W filament mounted behind the Ta plate. An exponential background has been removed from each TDS curve. The reading of the thermocouple has been calibrated (±5 K) in situ by TDS using the known heat of condensation of the alkanes (*n*-/isobutane,[29] *n*-pentane[33]). A heating rate of 1 K/sec has been used.

3. Results and Discussion

3.1. Sample Characterization − Distinguishing Closed- and Open-End CNTs. The CNT sample has been characterized by scanning electron microscopy (SEM) and thermal desorption spectroscopy (TDS), as summarized in Figure 1. SEM figures obtained before the ultrahigh vacuum (UHV) TDS experiments (Figure 1-I) show bright and dark lines which are CNTs deposited on the silica support (bright lines) and CNTs in a second layer (darker lines) on top of the first layer of CNTs. It is evident that the support is fully covered with little or no silica areas left bare. (See also the inset of Figure 1-I which shows SEM of a clean silica support.) SEM collected after the UHV experiments (Figure 1-II) indicates still a fully covered support.

As an additional confirmation that the data presented here are not obscured by support effects, *n*-pentane TDS of the

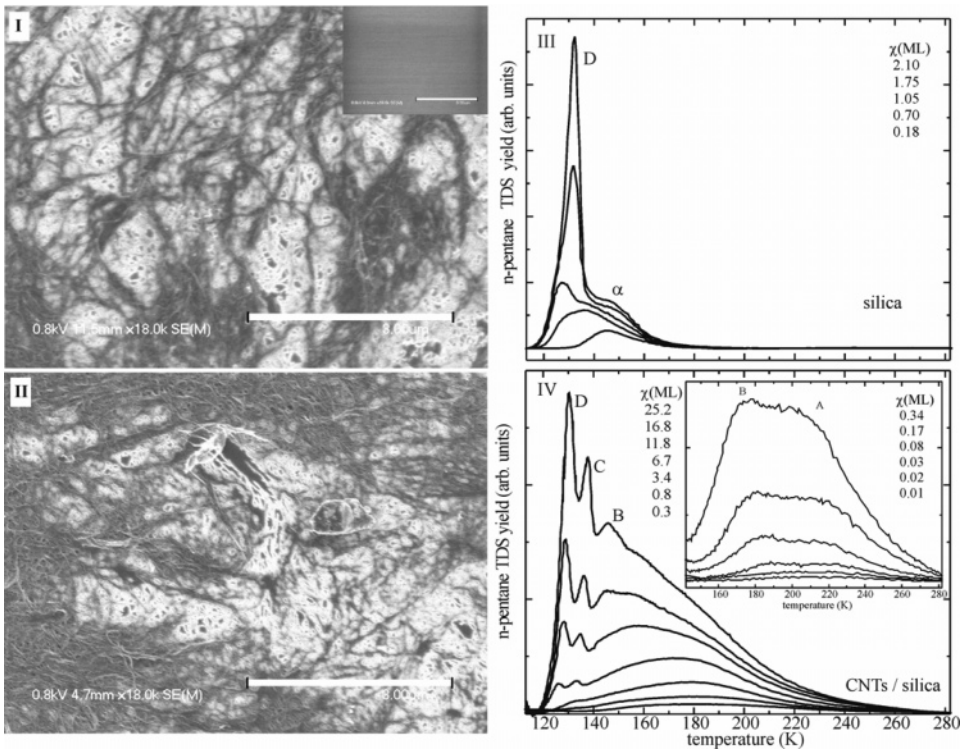

Figure 1. (I) Scanning electron microscopy (SEM) images of the carbon nanotubes (CNTs) on the silica support measured before the ultrahigh vacuum (UHV) experiments and **(**II) after the UHV experiments. All SEM images were obtained at an accelerating voltage of 0.8 kV. The scale bars represent 3 μm. The inset of (I) is the clean silica support. Two layers of CNTs can be seen in the images, a bottom layer (bright lines) and a top layer (dark lines). Thermal desorption spectroscopy (TDS) curves of *n*-pentane as a function of exposure (III) on the clean silica support (dosed by backfilling.) and (IV) on CNTs/silica. The latter results are in agreement with previous literature[33] and are presented as a consistency test. The labels assign the adsorption sites of the alkanes on the CNTs, (A) interior, (B) grove, and (C) exterior sites as well as (D) the condensation TDS peak.[33] The inset shows TDS data at small exposures (heating rate = 1 K/sec).

supported CNTs (Figure 1-IV) and of a clean silica support[32,45] (Figure 1-III) have been collected as a function of alkane exposure. These data sets look entirely different (Figure 1-III/IV). For the silica support, two TDS peaks are present (labeled as D and α). The leading edges of the low-temperature D peaks, observed at large exposures, line up, indicating zero-order kinetics and a condensation of the alkane. The α peak is already present at low exposures and shifts to lower desorption temperatures with increasing coverage, consistent with first-order molecular adsorption/desorption kinetics and repulsive lateral interactions. Both features are commonly observed for alkane adsorption.[26,32] In contrast, exposing *n*-pentane on the silica-supported CNTs leads to the observation of four distinct TDS structures which are labeled as A−D. The D peak is easily identified as a support-independent condensation peak since the leading edges line up. The C, B, and A TDS structures have been seen before for a variety of alkanes including *n*-pentane.[33] By means of adsorption-site-specific red shifts in infrared spectra and by determining filling factors, J. T. Yates et al.[33,46] could assign these structures to adsorption on interior (A), groove (B), and exterior (C) sites of the CNTs. Thus, TDS provides fingerprint spectra indicating, for example, the end termination of CNTs. Although some CNTs are in a second layer, adsorption in interstitials is only expected for very small adsorbates[43,47] (He, Ne, H), consistent with the TDS curves. The appearance of the A TDS peak corroborates that the CNTs, which have been sonicated and annealed for 15 min at 450 K in UHV, are open-end since alkane adsorption on interior sites is present. Furthermore, an exposure of 0.7 ML was sufficient to saturate the silica support, indicated by the onset of the condensation peak (Figure 1-III), whereas even 25 ML of *n*-pentane exposure did not lead to a clear saturation of the o-CNT monolayer (Figure 1-IV), which is in agreement with the expected enhancement in surface area.

Annealing temperatures above 600 K reduced the amount of CNTs on the silica support distinctly, as confirmed by SEM. In this case, TDS data characteristic of the bare silica support have been obtained. Apparently, the binding of the CNTs on silica is weaker than that for gold supports that could be flashed to significantly larger temperatures, which may result in a more efficient catalytic activation of the CNTs.[46] However, silica as a support has the advantage that aligned CNTs can be grown,[48] which could lead to anisotropy effects in molecular beam scattering studies. This may allow for the study of the dynamics of confinement effects. Furthermore, silica is a prototype support for the study of supported nanostructures.[49,50]

3.2. Adsorption Kinetics − Thermal Desorption Spectroscopy. TDS data for *n*-/isobutane on the CNTs are depicted in the left/right columns, respectively, of Figure 2. The upper row in Figure 2 shows data obtained from the as-prepared c-CNTs (see section 2.1) which have been degassed in UHV but have never been flashed above 300 K in UHV. The TDS data obtained for 450 K-annealed o-CNTs are shown in the center row. The data depicted in the bottom row directly compare results for o-CNTs (thick solid lines) with c-CNTs (thin solid lines) at small exposures.

TDS curves for c-CNTs are, at small exposures (see the insets of Figure 2), dominated by a featureless structure centered at 116 K for *n*-butane (at 112 K for isobutane). At large exposures, a condensation peak emerges (D peak). No further TDS peaks are present in the spectra. We assign the high-temperature structure to adsorption on outer adsorption sites of the c-CNTs (C peak), which are the smallest binding energy sites on CNTs (cf., Figure 1-IV).

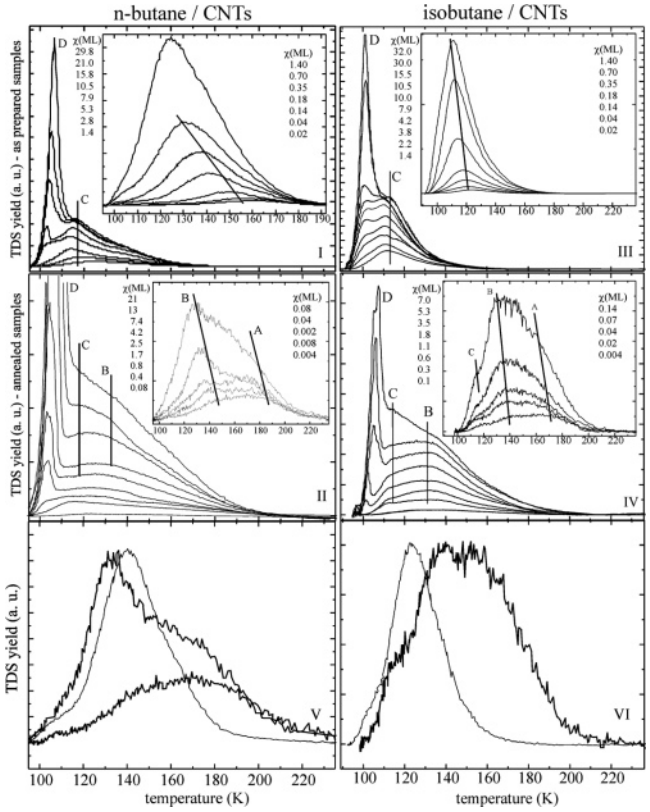

Figure 2. TDS measurements of the alkanes adsorbed on the CNTs as a function of exposure, χ, in ML (1 ML is defined as 1×10^{15} molecules/cm^2). Left column: *n*-butane. Right column: isobutane. Top row: as-prepared CNTs which have been degassed in vacuum but have never been flashed above 300 K. Center row: CNTs annealed at 450 K for 15 min. (The insets show TDS curves for low exposures. The labels assign adsorption sites; see Figure 1. Heating rate = 1 K/sec). Bottom row: direct comparison of TDS curves for o-CNTs (thick solid lines) and c-CNTs (thin solid lines). (Exposures: *n*-butane 0.04 and 0.004 ML for o-CNTs and 0.02 ML for c-CNTs; isobutane 0.02 ML for o-CNTs and c-CNTs.)

Annealing the CNT samples results in the appearance of two further TDS peaks at larger desorption temperatures and in a broadening of the curves. In agreement with previous work,[33] the peak at ~118 K is assigned to adsorption on exterior sites and the peak at ~130 K to adsorption of the alkanes on groove sites (cf., Figure 1-IV). A separation of the peaks is difficult, but it appears that the C and B peak positions depend only slightly on the isomer (at large exposures). Besides the condensation peak and within the range of small exposures, all TDS structures shift to lower desorption temperatures with increasing exposure (see the insets of Figure 2), indicating first-order kinetics and repulsive lateral interactions. Shifts in TDS peak positions due to lateral interactions are always[26] most distinct at small exposures (coverages), that is, no peak shifts are expected when approaching the saturation coverage. The peak positions given above refer to large exposures where the peaks are more clearly resolved. Assuming a pre-exponential factor of 1×10^{13}/sec leads to binding energies of 22.9 kJ/mol on exterior and of 33.6 kJ/mol on groove sites, respectively. The interior (highest binding energy) sites fill up first, which allows precise determination of the A peak position at small exposures; it amounts to 185 K for *n*-butane (170 K for isobutane), which corresponds to 47.7 kJ/mol (44.3 kJ/mol). The binding energies on interior sites for *n*-butane are slightly larger than those for isobutane, consistent with their geometrical structure and the physisorption of the alkanes.[26,32] On the bare silica support monolayer, TDS peak temperatures of 115/110 K have been determined for *n*-/isobutane at saturation, corresponding to 29.6/28.3 kJ/mol.[45] (We are not aware of kinetic data for butane on graphite surfaces.) Thus, consistent with earlier reports, a significant enhancement in binding energies is observed due to strong van der Waals interactions caused by the proximity of the curved nanotube walls.

We may add that CNT-induced TDS features appear to be more distinct for longer-chain alkanes; compare the TDS curves in Figures 1-IV and 2, which have been collected on subsequent measuring days. This may simply be related to the smaller binding energies of smaller alkanes as compared with longer-chain alkanes. Thus, all TDS features overlap more strongly for short-chain alkanes. Therefore, the pentane data show even more clearly than the butane data that the annealed CNTs were open end. Figure 2-V/VI, which presents a direct comparison of o-CNTs and c-CNTs TDS data, clearly shows, however, that the A TDS peak is present for the annealed CNTs but not for the as-prepared CNTs. (Longer-chain alkanes are liquids at standard conditions, which makes it very difficult to generate a molecular beam, particularly when variable impact energy is important.)

The c-CNTs must already be fairly clean, which allows the study of the effect of opening the entry ports of the CNTs on the adsorption dynamics by comparing results obtained for the as-prepared and annealed CNTs. (1) The position of the C peak agrees well with the one obtained for the annealed o-CNTs; a coadsorption with impurities should alter the binding energy of the alkanes via lateral interactions. (2) If the c-CNTs were covered entirely with solvent residuals, no clear separation of the D and C peaks would be expected, as seen for contaminated TiO_2 nanotube samples.[51] However, the absence of the A and B structures for as-prepared CNTs shows that the tube ends are blocked by functionalities. Note also the increase in the intensity, mostly at the A and B peak positions, after annealing the CNTs, which leads to the broadening of the TDS curves. (3) It appears that the C peak structures for c-CNTs saturate (Figure 2-I/II). Comparing TDS peak areas for c-CNTs and those for the silica support leads to an estimated enhancement of the surface area by a factor of 40, which corresponds to ~20 m^2/g for the ~200 μg sample studied. This surface area is consistent with literature reference data, which indicate 38 m^2/g for Ne adsorption on c-CNTs.[43,47]

3.3. Adsorption Dynamics — Molecular Beam Scattering. *a. Example of an Adsorption Transient.* An example of adsorption transients (alkane pressure in the scattering chamber vs exposure time) of o-CNTs (thick solid line) and c-CNTs (thin solid line) is shown in Figure 3. The opening of the beam flag defines the zero point on the exposure time scale. The background has been normalized to zero and the saturation level to one, that is, the intensity scale corresponds to 1-*S*. As is evident, the initial adsorption probability, S_0, is larger for o-CNTs than for c-CNTs. Furthermore, the area above the transient and below the saturation level (which equals the saturation coverage) is larger for o-CNTs than for c-CNTs. The c-CNT/o-CNT ratio of these areas amounts approximately to 0.4. Opening the tube ends should enhance the monolayer adsorption capacity of the samples by not more than a factor of 2. Thus, the adsorption transients indicate that the annealed CNTs are fairly clean, consistent with the TDS data.

b. Initial Adsorption Probabilities (S_0) — Impact Energy Dependence. The impact energy dependence of S_0 for *n*-/isobutane adsorption on c-CNTs (open symbols) and o-CNTs (closed symbols) just above the condensation temperature is depicted in Figure 4-I. The lines are a parametrization of the

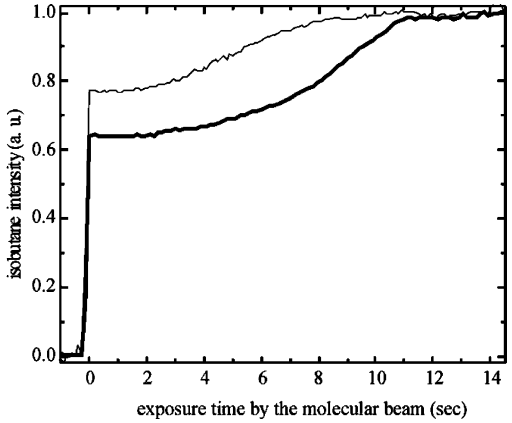

Figure 3. Example of adsorption transients, that is, the isobutane pressure in the scattering chamber of the beam system versus exposure time by a 3% isobutane beam (balance He) is shown. The thick solid line is for o-CNTs ($E_i = 0.74$ eV); the thin solid line is for c-CNTs ($E_i = 0.85$ eV). The transients normalized as 1 − adsorption probability versus exposure time are shown ($T_{ads} = 112$ K).

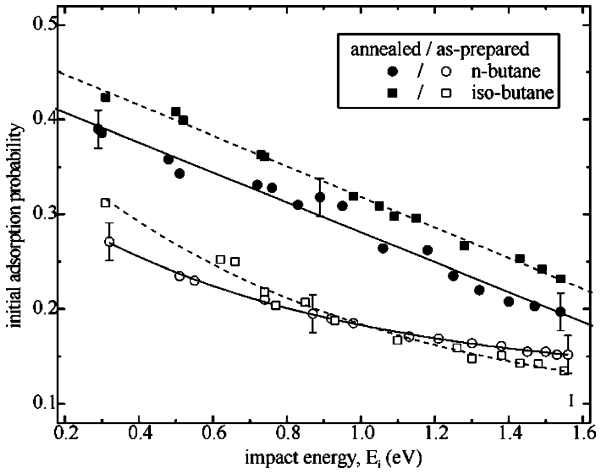

Figure 4. Illustrated is the enhancement in the initial adsorption probability, S_0, of the alkanes by opening the CNT entry ports. Depicted is S_0 as a function of impact energy, E_i, and at a surface temperature, T_{ads}, of ~110 K, that is, slightly above the condensation temperature of the alkanes. Data for all alkanes studied (as-prepared/UHV-cleaned CNTs) are shown. The curves have been parametrized by a best fit procedure (*n*-butane: annealed $S_0 = -0.15E_i + 0.44$; as-prepared $S_0 = 0.39\exp(-E_i/0.36) + 0.12$; isobutane: annealed $S_0 = -0.16E_i + 0.48$; as-prepared $S_0 = 0.56\exp(-E_i/0.37) + 0.08$ with E_i in eV).

curves (see the figure caption), which are included as a guide for the eye. Note that one advantage of the King and Wells technique for measuring adsorption probabilities is that it does not require any calibrations (e.g., flux, coverage) to obtain absolute S_0 values.

Most importantly, opening the tube ends leads to an increase in S_0 by 0.12 ± 0.04 (31%) at $E_i = 0.31$ eV, nearly identical for both *n*- and isobutane. S_0 is the ratio of adsorbed to exposed particles. Thus, increasing the number of possible adsorption sites by opening the tubes should increase S_0, as is observed. This effect is the opposite of the commonly observed site blocking effect in coadsorption studies where S_0 decreases with the decreasing number of available adsorption sites (due to site blocking by the coadsorbate).[52,53] An enhancement in S_0 by opening the tube ends also has been determined (by TDS) for Xe adsorption on o-CNTs.[21] In the case of Xe, a quasi-one-dimensional phase transition has been proposed according to the observed zero-order kinetics (TDS peak shifts to larger temperatures with increasing exposure). Since the TDS peak

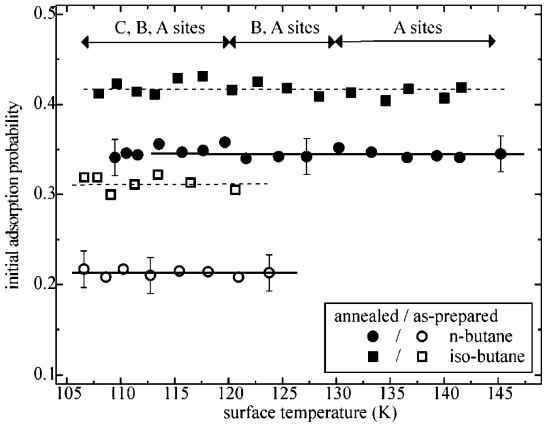

Figure 5. Temperature dependence of the initial adsorption probability of *n*-/isobutane adsorbed on the CNTs (annealed/as-prepared). ($E_i = 0.74$ eV for *n*-butane, and $E_i = 0.31$ eV for isobutane.) The arrows indicate the temperature range where the different adsorption sites on the CNTs are kinetically favored.

positions for butane shift in the opposite direction (see Figure 2), physisorption of butane on interior sites and first-order kinetics are concluded.

The decrease in S_0 with increasing impact energy (Figure 4) is consistent with smaller trapping probabilities at large impact energies. This result has commonly been obtained for molecular adsorption on planar catalysts.[40] At large E_i, more energy needs to be dissipated to the surface in order to adsorb the gas-phase species, that is, S_0 decreases with E_i.

We may expect anisotropy effects in beam scattering experiments on o-CNTs. Therefore, we collected S_0 data for constant E_i but at different impact angles, α_i. However, total energy scaling was observed, that is, S_0 was independent of α_i.[40,54]

c. Initial Adsorption Probabilities — Temperature Dependence. The temperature dependence of S_0 at large and small E_i's (see the figure captions) is shown in Figure 5. S_0 is distinctly larger for the open-end CNTs, as discussed above. Consistent with nonactivated molecular adsorption is the independence of S_0 from the adsorption temperature, T_{ads}. In other words, the $S_0(T_{ads})$ curves are featureless, as commonly observed for alkane adsorption.[26] Although adsorption of the alkanes on internal sites is kinetically favored within 130−145 K (see the arrows in Figure 5), S_0 does not change with T_{ads}. This result is expected since the "landing sites" (C or B sites) of the alkanes are identical within the entire temperature range, that is, independent of the final and kinetically favored (determined by T_{ads}) adsorption site (i.e., A sites for $130 < T_{ads} < 145$ K).

d. Coverage-Dependent Adsorption Probabilities. The coverage dependence of the adsorption probability is shown in Figure 6. The left column depicts *n*-butane and the right one isobutane $S(\Theta)$ data. Whereas the top row data are obtained for c-CNTs, the bottom row curves are for o-CNTs. E_i has been varied, as indicated, and T_{ads} is set to a temperature just above the condensation of the alkanes. The absolute coverage of the alkanes for o-CNTs and c-CNTs will certainly be different,[43,47] but the saturation coverages are normalized to 1, allowing for a better comparison of the curve shapes. For both c-CNTs and o-CNTs, precursor-mediated adsorption is present since, in the absence of precursor states, $S(\Theta)$ decreases linearly with Θ, in contrast to the measured shape of $S(\Theta)$. The detected $S(\Theta)$ curves have a typical Kisliuk-like shape. However, $S(\Theta)$ for c-CNTs decreases faster with increasing coverage than that for the o-CNTs, that is, the initial slope of the $S(\Theta)$ curves is smaller for c-CNTs than that for o-CNTs at comparable E_i's. (This result would be even more distinct if the absolute coverages would

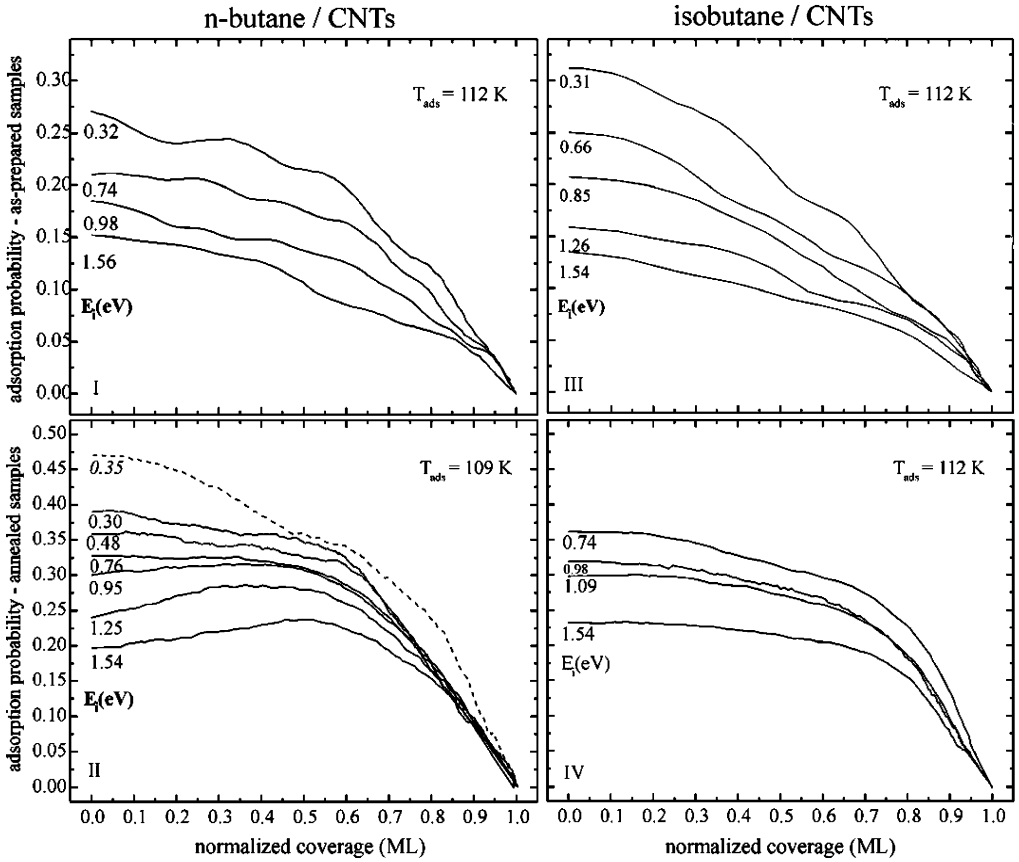

Figure 6. Coverage dependence of the adsorption probability parametric in impact energy, E_i, and at an adsorption temperature just above the condensation temperature of the alkanes, as indicated. Left column: n-butane. Right column: isobutane data. Top row: as-prepared CNTs. Bottom row: annealed CNTs. (The dashed line in panel II is for *n*-pentane adsorption at $T_{ads} = 135$ K.)

be taken into account.) At a given surface temperature, the lifetime of the precursor state will be identical for o-CNTs and c-CNTs. Thus, the flatter $S(\Theta)$ curves for o-CNTs are consistent with an enhancement in the trapping probabilities, which is again a result of the larger active surface area of o-CNTs. (Note that the $S(\Theta)$ curves in Figure 6 show an increase in S with coverage (adsorbate-assisted adsorption) at large E_i, which is caused by a slightly smaller adsorption temperature (larger coverage) in this data set.[26])

4. Conclusions and Summary

The first molecular beam scattering study on a nanotube system, CNTs supported on silica, is reported. The following information has been gathered.

The thermal desorption spectroscopy (TDS) curves for annealed CNTs (o-CNTs) consist of four structures which can be assigned to adsorption on interior (A), groove (B), and exterior (C) sites as well as condensation of the alkanes (D peak), as observed before for longer-chain alkanes. Whereas exterior sites are resolved for as-prepared CNTs (c-CNTs), the TDS features characteristic of internal adsorption sites are missing. Molecular adsorption/desorption kinetics (first-order) are observed with high-energy binding sites present on the CNTs as compared with a planar silica surface. Opening the tube ends leads to an increase in the initial adsorption probability, S_0, which is approximately identical for *n*-butane and isobutane. This effect is consistent with the enhancement in surface area by opening the tube ends. S_0 decreases with impact energy, reflecting the decrease in the efficiency in gas−surface energy transfer processes with increasing E_i. Total energy scaling is observed for S_0. S_0 is independent of adsorption temperature, indicating nonactivated and precursor-mediated adsorption dynamics. Finally, the coverage-dependent adsorption probabilities, $S(\Theta)$, for both c-CNTs and o-CNTs are consistent with precursor-mediated adsorption. However, the initial slope of the $S(\Theta)$ curves at comparable impact energies for c-CNTs is smaller than that for o-CNTs, indicating an enhancement in trapping probabilities by opening the tube entry ports.

Acknowledgment. Assistance in the final stage of the project by J. Goering (Fargo) is acknowledged. Financial support by DoE-ND-EPSCoR (DE-FG02-06ER46292, state grant) and from ND−NSF-EPSCoR IIP seed (EPS-047679) is acknowledged by NDSU. The authors at Columbia would like to thank the National Science Foundation (Grant CHE-04-15516) for generous support of this research and relied on equipment supported by the NSEC program of the National Science Foundation under Award Number CHE-0117752, NSF-CHE-04-15516 and by the New York State Office of Science, Technology, and Academic Research (NYSTAR). We are grateful to the late Professor R. E. Smalley for a gift of HiPco tubes.

References and Notes

(1) Iijima, S. *Nature* **1991**, *354*, 56.
(2) Vigolo, B. *Science* **2002**, *290*, 1331.
(3) Arab, M.; Picaud, F.; Devel, M.; Ramseyer, C.; Girardet, C. *Phy. Rev. B* **2004**, *69*, 165401.
(4) Kong, J.; Franklin, N.; Zhou, C.; Chapline, M.; Peng, S.; Cho, K.; Dai, H. *Science* **2000**, *287*, 622.
(5) Dillon, A. C.; Jones, K. M.; Bekkendahl, T. A.; Kiang, C. H.; Bethune, D. S.; Heben, M. J. *Nature* **1997**, 386, 377.
(6) Talapatra, S.; Migone, A. D. *Phys. Rev. Lett.* **2001**, *87*, 206106.
(7) Tans, S. J.; Verschueren, A. R. M.; Dekker, C. *Nature* **1998**, *393*, 49.

(8) Tans, S. J.; Verschueren, A. R. M.; Dekker, C. *Nature* **1998**, *393*, 49.
(9) Yao, Z.; Postma, H. W. C.; Balents, L.; Dekker, C. *Nature* **1999**, *402*, 273.
(10) Bing, Z., Hermans, S., Somorjai, G. A., Eds. *Nanotechnology in Catalysis*; Springer Series: Nanostructure Science and Technology; Springer: New York, 2004.
(11) Planeix, J. M.; Coustel, N.; Coq, B.; Brotons, V.; Kumbhar, P. S.; Utartre, R. D.; Eneste, P. G.; Ernier, P. B.; Alayan, P. M. *J. Am. Chem. Soc.* **1994**, *116*, 7935.
(12) Burghard, M. *Surf. Sci. Rep.* **2005**, *58*, 1.
(13) Carmo, M.; Paganin, V. A.; Rosolen, J. M.; Gonzalez, E. R. *J. Power Sources* **2005**, *142*, 169.
(14) Dicks, A. L. *J. Power Sources* **2006**, *156*, 128.
(15) Chin, Y.; Hu, J.; Cao, C.; Gao, Y.; Wang, Y. *Catal. Today* **2005**, *110*, 52.
(16) Bahome, M. C.; Jewell, L. L.; Hildebrandt, D.; Glasser, D.; Coville, N. J. *Appl. Catal., A* **2005**, *287*, 60.
(17) Muris, M.; Dupont-Pavlovsky, N.; Beinfait, M.; Zeppenfeld, P. *Surf. Sci.* **2001**, *492*, 67.
(18) Kondratyuk, P.; Yates, J. T. *Chem. Phys. Lett.* **2004**, *383*, 314.
(19) Ulbricht, H.; Moos, G.; Hertel, T. *Surf. Sci.* **2003**, *532*−*535*, 852.
(20) Byl, O.; Liu, J. C.; Wang, Y.; Yim, W. L.; Johnson, J. K.; Yates, J. T. *J. Am. Chem. Soc.* **2006**, *128*, 12090.
(21) Kuznestsova, A.; Yates, J. T.; Liu, J.; Samalley, R. E. *J. Chem. Phys.* **2000**, *112*, 9590.
(22) Lei, R. Z.; Gellman, A. J.; Koel, B. E. *Surf. Sci.* **2004**, *554*, 125.
(23) Paserba, K. R.; Gellman, A. J. *Phys. Rev. Lett.* **2001**, *86*, 4338.
(24) Paserba, K. P.; Gellman, A. J. *J. Chem. Phys.* **2001**, *115*, 6737.
(25) Slayton, R. M.; Aubuchon, C. M.; Camis, T. L.; Noble, A. R.; Tro, N. J. *J. Phys. Chem.* **1995**, *99*, 2151.
(26) Wang, J.; Hokkanen, B.; Burghaus, U. *Surf. Sci.* **2006**, *600*, 4855.
(27) Brand, J. L.; Arena, M. V.; Deckert, A. A.; George, S. M. *J. Chem. Phys.* **1990**, *92*, 5136.
(28) Funk, S.; Hokkanen, B.; Wang, J.; Burghaus, U.; Bozzolo, G. H.; Garces, J. E. *Surf. Sci.* **2006**, *600*, 583.
(29) Xu, C.; Koel, B. E.; Paffett, M. T. *Langmuir* **1994**, *10*, 166.
(30) Funk, S.; Nurkic, T.; Burghaus, U. *Appl. Surf. Sci.* **2007**, *253*, 4860.
(31) Wang, J.; Hokkanen, B.; Burghaus, U. *Surf. Sci.* **2005**, *577*, 158.
(32) Funk, S.; Nurkic, T.; Burghaus, U. *Appl. Surf. Sci.* **2006**, *253*, 4860.
(33) Kondratyuk, P.; Wang, Y.; Johnson, J. K.; Yates, J. T. *J. Phys. Chem. B* **2005**, *109*, 20999.
(34) Ding, J.; Burghaus, U.; Weinberg, W. H. *Surf. Sci.* **2000**, *446*, 46.
(35) Kuznetsova, A.; Popova, I.; Yates, J. T.; Bronikowski, M. J.; Huffman, C. B.; Liu, J.; Smalley, R. E.; Hwu, H. H.; Chen, J. G. *J. Am. Chem. Soc.* **2001**, *123*, 10699.
(36) O'Connell, M. J.; Bachilo, S. M.; Huffman, C. B.; Moore, V. C.; Strano, M. S.; Haroz, E. H.; Rialon, K. L.; Boul, P. J.; Noon, W. H.; Kittrell, C.; Ma, J. P.; Hauge, R. H.; Weisman, R. B.; Smalley, R. E. *Science* **2002**, *297*, 593.
(37) Dukovic, G.; White, B. E.; Zhou, Z.; Wang, F.; Jockusch, S.; Steigerwald, M. L.; Heinz, T. F.; Friesner, R. A.; Turro, N. J.; Brus, L. E. *J. Am. Chem. Soc.* **2004**, *126*, 15269.
(38) Geng, H. Z.; Zhang, X. B.; Mao, S. H.; Kleinhammes, A.; Shimoda, H.; Wu, Y.; Zhou, O. *Chem. Phys. Lett.* **2004**, *399*, 109.
(39) Yim, W. L.; Byl, O.; Yates, J. T.; Johnson, J. K. *J. Chem. Phys.* **2004**, *120*, 5377.
(40) Wang, J.; Burghaus, U. *J. Chem. Phys.* **2005**, *122*, 044705-11.
(41) King, D. A.; Wells, M.G. *Surf. Sci.* **1972**, *29*, 454.
(42) Yates, J. T. *Experimental Innovations in Surface Science: A Guide to Practical Laboratory Methods and Instruments*; Springer-Verlag: New York, 1998.
(43) Krungleviciute, V.; Heroux, L.; Talapatra, S.; Migone, A. D. *Nano Lett.* **2004**, *4*, 1133.
(44) Byl, O.; Liu, J.; Yates, J. T. *Langmuir* **2005**, *21*, 4200.
(45) Funk, S.; Burghaus, U. In preparation.
(46) Kondratyuk, P.; Yates, J. T. *Chem. Phys. Lett.* **2005**, *410*, 324.
(47) Talapatra, S.; Zambano, A. Z.; Weber, S. E.; Migone, A. D. *Phys. Rev. Lett.* **2000**, *85*, 138.
(48) Huang, L. M.; Cui, X. D.; White, B.; O'Brien, S. P. *J. Phys. Chem. B* **2004**, *108*, 16451.
(49) Kwon, S.; Yan, X.; Contreras, A. M.; Liddle, J. A.; Somorjai, G. A.; Boker, J. *Nano Lett.* **2005**, *5*, 2557.
(50) Johanek, V.; Laurin, M.; Grant, A. W.; Kasemo, B.; Henry, C. R.; Libuda, J. *Science* **2004**, *304*, 1639.
(51) Funk, S.; Hokkanen, B.; Burghaus, U.; Ghicov, A.; Schmuki, P. *Nano Lett.* **2007**, *7*, 1091.
(52) Burghaus, U.; Ding, J.; Weinberg, W. H. *Surf. Sci.* **1997**, *384*, L869.
(53) Funk, S.; Burghaus, U. *Phys. Chem. Chem. Phys.* **2006**, *8*, 4805.
(54) Darling, G. R.; Holloway, S. *Rep. Prog. Phys.* **1995**, *58*, 1595.